



두 개의 동일한 타원형 구조를 지닌 광 도파관의 특성

장성호* · 정상호** · †이승환*,***

한국교통대학교 기계공학과, 한국교통대학교 산학협력단, 한국교통대학교 지역혁신센터(RIC)
(2014년 3월 31일 접수, 2014년 4월 25일 수정, 2014년 4월 25일 채택)

Characteristics of an Optical Waveguide with Two Identical Elliptical Structures

SeongHo Jang* · SangHo Chung** · †SeungHwan Yi*,***

*Department of Mechanical Eng., KNUT (Korea National University of Transportation),
Chungjushi, Chungbuk 380-702, Rep.of Korea

**Industry-Academic Cooperation Foundation, KNUT, Chungjushi, Chungbuk 380-702,
Rep.of Korea

***RIC(Regional Innovation Center), KNUT, Chungjushi, Chungbuk 380-702, Rep.of Korea
(Received March 31, 2014; Revised April 25, 2014; Accepted April 25, 2014)

요 약

본 논문에서는 알코올 측정용 센서의 광학적 특성 향상을 위한 고유한 광학적 구조를 제안하였으며, 모의해석을 실시하였다. 광 도파관은 한쪽에 공통초점을 갖는 두 개의 타원형 광 도파관으로 구성되었으며, 각 광 도파관의 서로 다른 초점에 적외선 광원과 적외선 센서를 갖는다. 두 타원형 광 도파관의 각도가 30도에서 90도로 증가시켰을 때, 단위면적당 최대 입사광량은 $2.23 \times 10^6 \text{ W/m}^2$ 에서 $5.74 \times 10^5 \text{ W/m}^2$ 로 감소하였다. 그러나 조사 빔의 반지름은 1.86 mm로 최소값을 나타내었고, 전체 입사 에너지는 90도 각도를 갖는 구조와 비교하여 약 10% 작은 값을 보였다. 모의해석 결과로부터 본 논문에 제안한 구조는 긴 흡수파장을 갖는 광학적 가스센서의 감도향상에 기여할 것으로 판단된다.

Abstract - A unique optical waveguide structure is proposed to enhance the optical characteristics of alcohol screening sensors. This structure is then simulated. The structure consists of two elliptical waveguides that have a common focus to one side and has an IR source and detector at each of the other focal points of the ellipses. When the angle between the two elliptical waveguides is increased from 30 degrees to 90 degrees, the maximum level of irradiance is greatly decreased, falling from $2.23 \times 10^6 \text{ W/m}^2$ to $5.74 \times 10^5 \text{ W/m}^2$. However, the diameter of the incident rays is at a minimum of 1.86mm and the total incident flux is less than 10% lower when compared to the structure at 90°. It can be seen from the simulation results that this structure might enhance the sensitivity of an optical gas sensor which has a large absorption wavelength.

Key words : elliptical waveguide, NDIR gas sensor, thermopile output voltage, maximum irradiance

†Corresponding author: isaac_yi@ut.ac.kr

Copyright © 2014 by The Korean Institute of Gas

I. INTRODUCTION

Following the invention and commercialization of semiconductor gas sensors five decades ago, there was a great deal of work to improve the performance of the gas sensors[1-3]. The three types of gas sensors that have been widely used in domestic, industrial and also automotive areas, are semiconductor, catalytic, and electrochemical cell based units[4-6]. Since the principles of the above mentioned sensors are based upon the chemical reactions between the target gas and the surface of the sensor, they are heated up to activate the surfaces of the sensors in order to improve the sensitivity of the sensor itself. However, these devices show poor selectivity amongst other ambient gases (mainly water vapor, hydrocarbons, and other environmental gases) because the surfaces are exposed directly to the environment[7-8]. Even though there are some technical methods to improve the selectivity of the sensors, there are still huge challenges to discriminate the target gas from other ambient gases in field applications.

Approximately one decade ago, the NDIR (Non-Dispersive Infrared Rays) principle was applied to sensors for ear thermometers, home and office automation regions with silicon thermopiles or PIR (Passive InfraRed) detectors[9-10]. Because these use IR filters in order to detect temperature and gases, they can enhance the selectivity that hinders the improvement of gas sensors. Furthermore, gas sensors that use the NDIR principle alleviate the contamination of the sensors and increase the sensitivity, reliable operating period, and accuracy without deterioration of the selectivity. There is therefore a shift from ceramic gas sensors to optical gas sensors in some specific gas sensor applications.

Currently, alcohol sensor systems are becoming popular, not only for the screening of drunken drivers, but also for built-in alcohol lock systems, in order to prohibit DWI (Driving While Intoxicated). The dominant sensor technology at present for alcohol sensors or screening devices is based upon catalytic combustion, either with a fuel cell or heated metal oxide ceramics. However, due to the degradation of heating elements and potential contamination of the sensor surfaces by polluted air,

the reliability and long term stability are major issues with both sensor types. These devices also need a cumbersome calibration process after several months of operation. There has been a push therefore for sensing technology and devices using robust and reliable NDIR sensing principles[11]. One of the main components in this technology is the optical waveguide, with a unique structure and also small feature size, since both the IR source and detector have been well developed and stabilized in order to realize NDIR gas sensors.

In order to build and provide an alternative alcohol sensor using the NDIR principle, analysis of patents has been executed to propose a unique optical waveguide and simulate its operation using commercial software, and present its optical characteristics in this paper.

II. PRINCIPLE CONCEPTS AND MODELING

2.1. Principle concepts of a NDIR gas sensor

In an elliptical waveguide structure, when light radiates from one focal point, it reflects on the mirrored inside surfaces of the elliptical structure until it reaches the other focal point. If the mirrored surfaces reflect whole rays that are directed perfectly at one focal point, whole rays will reach the other focal point without any loss.

When this structure is applied to a NDIR gas sensor, the radiated beams at one focal point will be governed by the Beer-Lambert law, which describes the absorption of radiation energy by gas molecules with geometric dimensions:

$$I_d = I_0 \exp(-a \cdot x \cdot l) \quad (1)$$

where I_0 is the irradiance of light at the source [W/m^2], I_d is the irradiance of light at the detector [W/m^2], a is the absorption coefficient of the molecule, x is the concentration of molecules of gas, and l is the optical traveling length [m] from the source to the detector.

Eq. (1) presents the relationship between the optical irradiance and geometric factors. If the characteristics of the target are well known, the received light intensity will be determined by the gas

concentration and the optical path length. Therefore, the optical travelling length should be enlarged to increase the sensitivity of the sensor in the limited conditions.

When the focused bundle of the radiation beam is considered, the output voltage can be described by Eq. (2)[12]

$$V = \zeta (r_i/r_s)^2 \cdot \exp(-a \cdot x \cdot l) \quad (2)$$

where ζ is a proportionality constant that includes the reflection coefficient of the coating material of the optical waveguide, r_i is the radius of the beam of the IR ray, and r_s is the radius of the focused beam in the waveguide structure.

As can be inferred from Eq. (2), the output voltage can be enhanced by the square of the beam radius ratio between r_i and r_s . This means that the sensitivity of a NDIR gas sensor might be increased by focusing the radiated beam at the detector.

2.2. Modeling and Simulation

The performance of a NDIR gas sensor might be enhanced by varying two factors, the optical path length and the diameter of the incident rays, as described in Eq. (1) & (2). A longer optical path length can be achieved using a long cylindrical structure, or by multiple reflections of light within a small waveguide[13,14]. The focusing of light can be satisfied using an optical lens[15] or curved-

mirror structure[12]. However, the optical lens will increase the cost of materials and also the number of manufacturing steps, therefore it would be better to focus the beam without any redundant parts. As a result of these considerations, a novel optical waveguide that has two elliptical structures is proposed as shown in Fig. 1.

Generally, when the light is emitted from one focal point in ellipse, it reflects once at the inside of elliptical mirror surface and then it reaches to the other focal point. If the mirror is a perfect reflector, the emitted light energy could be focused at the other focal point. So the energy density could be increased tremendously and enlarge the output voltage of IR sensor. Therefore the sensitivity might be improved effectively. By using this fundamental principle, the proposed optical waveguide, as shown in Fig.1, consists of two identical ellipses that have a common focal point at one side (right-side, A_2). At the other two focal points an IR source (left upper: A_1) and an IR detector (lower left-side: A_5) are located in order to increase the optical path length and focus the incident rays onto the IR detector. The lengths of the major and minor axes in the ellipses are 100 mm and 40 mm, respectively. The properties of the IR source, detector and mirror surfaces are assumed to be as follows; the IR source type is a Lambertian disc with 5,000 rays and 10 watts at a wavelength of 3.4 μ m, the detector absorbs the incident beam perfectly and the reflectance of the mirror surfaces is 0.95. The diameter and thickness of the Lambertian disc are 1mm and 0.05mm, and the detector has a 16 mm diameter with a thickness of 0.05mm.

After modeling the elliptical waveguide using a 3-D CAD tool named Pro-E[®], the 3-D model was converted by Trace-Pro[®] in order to construct the optical structures of the elliptical waveguide. Then the parameters of each component (mirror surfaces, IR source, and IR detector) were input in order to simulate the characteristics of the elliptical waveguide according to the angle between the two major axes in the ellipses. The proposed optical waveguide has an opened area that is not covered by original ellipse, so the light that transits a common

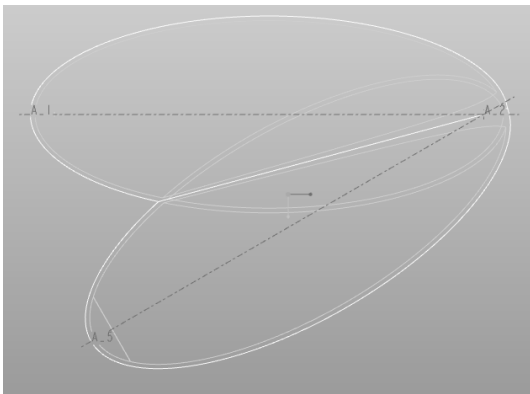


Fig. 1. Schematics of 2-dimensional optical waveguide with two ellipses.

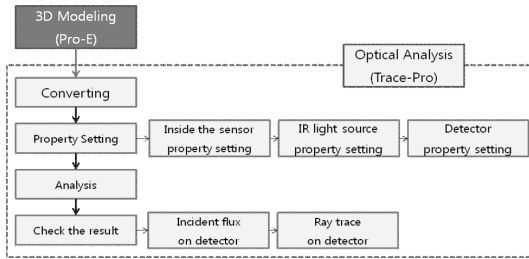


Fig. 2. Schematics of the simulation processes.

focal point might affect the trajectory of the light after passing it. Therefore the optical characteristics should be analyzed according to the angle between two major axes in optical waveguide. The simulation processes are depicted in Fig. 2.

III. SIMULATION RESULTS AND DISCUSSION FOR THE ELLIPTICAL WAVEGUIDE

The ray tracing inside of the elliptical waveguide is shown in Fig. 3. The IR radiation from the source (the first focal point located at the upper-left side) travels inside the structure and the bundle of rays passes a common focal point to the nearest mirror surfaces, from where it is reflected to reach the detector located at the lower-left side of the cavity. In this simulation, the number of rays was assumed to be 100 in order to reveal the trajectory of light. As can be seen in Fig. 3 a), there is significant irregular scattering, which is due to the imperfect ellipses at the center of the two elliptical waveguides. However, the irregular scattering has almost been eliminated in Fig. 3 b) and this is as a result of the small overlapping area between the first and the second ellipses. Furthermore, even though incoming light passes through the common focus, the light changes trajectory after passing through and so the light reflects at an abnormal mirror surface as shown at the upper right corner, and then disperses onto the detector side that is located at the lower part as can be seen in Fig. 3 b).

Figure 4 shows the incident rays as a function of the angle between the two elliptical waveguides. When the angle between the two elliptical waveguides was 30 degrees, the incident ray count was 4,549 rays. However, when the angle was increas-

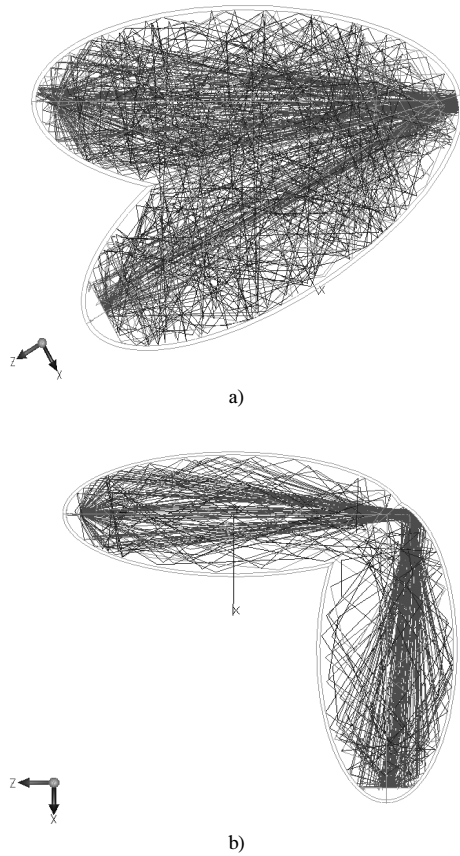


Fig. 3. Ray tracing within the elliptical waveguide: (a) 30°, (b) 90° with 100 rays.

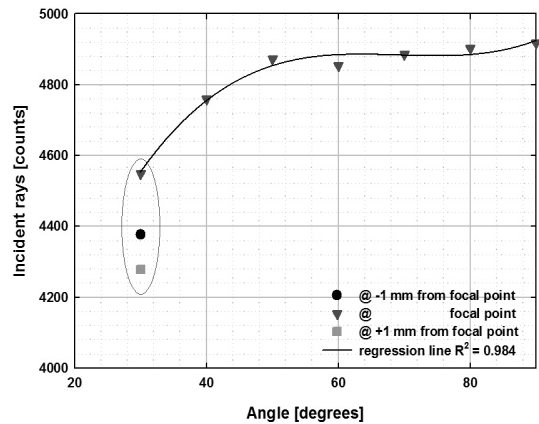


Fig. 4. Incident rays as a function of the angle between the two elliptical waveguides.

ed, the ray count also increased to 4,800 rays at 60 degrees and then saturates at around 4,900 rays at 90 degrees. This means that the quantity of IR light diminishes with a decreasing angle and this might be caused by multiple scatterings on the inside of the elliptical waveguide due to the enlargement of the imperfect ellipses.

The maximum irradiance as a function of angle is shown in Fig. 5. When the angle between the two elliptical waveguides is 30 degrees, the irradiance is $2.23 \times 10^6 \text{ W/m}^2$. However, as the angle is enlarged, the maximum irradiance decreases by approximately one order of magnitude at 90 degrees, with an irradiance of $5.74 \times 10^5 \text{ W/m}^2$. The maximum irradiance for one elliptical waveguide is $9.29 \times 10^6 \text{ W/m}^2$, and there is no elimination of radiated light on the detector. When the results mentioned above are compared, the maximum irradiance is decreased by a factor of 4 and one order of magnitude, respectively. This may be due to the enlargement of the open areas of the elliptical waveguide, which causes imperfect reflection of the incident rays onto the mirror surfaces, before and after passing the common focal point. This could also be potentially caused by the absence of a reflecting mirror near to the focal point for the radiated beam from the IR source.

The incident rays and also the maximum irradiance are also presented when the IR source is out of focus from the focal point as shown in Fig. 4

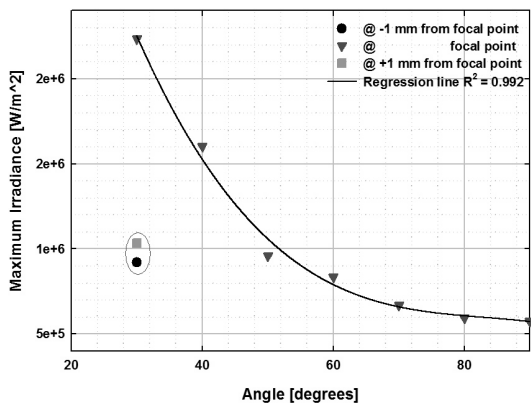


Fig. 5. Maximum irradiance as a function of the angle between the two elliptical waveguides.

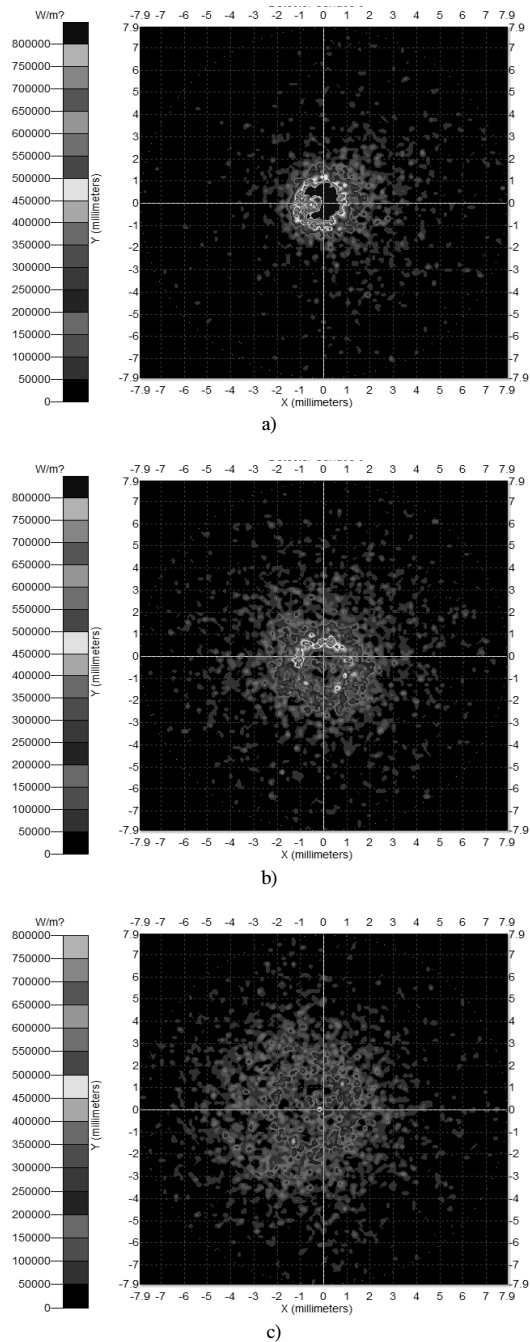


Fig. 6. Irradiance maps of incoming IR light onto the detector according to the angles between the two elliptical waveguide: a) 30°, b) 60°, and c) 90°.

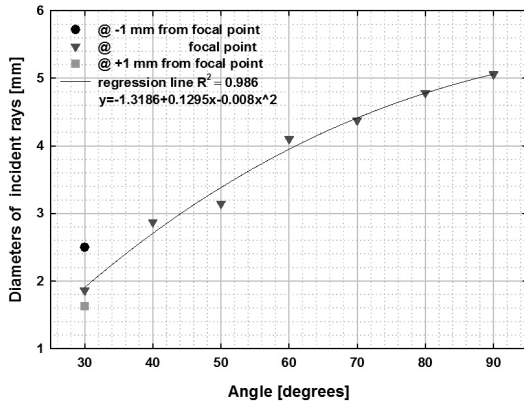


Fig. 7. Diameter of the incident rays as a function of the angle between the two elliptical waveguides.

and Fig. 5. In this case, the incident ray count is more than 10% lower than that for a perfectly aligned structure and the maximum irradiance is approximately the same as when there is a 50 degree angle between the two elliptical waveguides.

Figure 6 shows an irradiance map of the incoming IR light according to the angle between the two elliptical waveguides.

The dotted circle represents the periphery of the detector and the color indicates the irradiance of light. As can be seen in Fig. 6, when the angle is 30 degrees, the incoming light is focused onto a small spot of around 2mm diameter. However, when the angle is enlarged to 60 or 90 degrees, the irradiance of incoming lights shows the dispersed mapping also regions where the IR light cannot reach the detector. This might be understood by the enlargement of the abnormal trajectories and mirror surfaces. As a result of these factors the IR light passing through the common focus travels in a different path and exhibits patchy and dispersed light distributions on the detector.

The diameters of the incident rays on the detector are shown in Fig. 7. Due to the effects mentioned earlier, the diameters of the incident rays increase with an increase in the angle between the two elliptical waveguides. The diameter of the incident rays shows a smaller spot size when they are +1mm from the focal point, however, the maximum irradiance is slightly less than a factor of

two lower as shown in Fig. 5.

IV. CONCLUSIONS

In this study, the irradiance of IR rays, incident rays and the diameters of the incident rays are simulated with two identical elliptical cavity structures. Despite the fact that the incident ray count is increased with an increase of the angle between the structures, the maximum irradiance is drastically decreased and shows a scattered pattern of a large diameter.

In conclusion, it is efficient to decrease the angle between the two elliptical cavity structures in terms of the irradiance and the diameters of the incident rays in order to enhance the performance of the optical characteristics in optical sensor applications.

Acknowledgements

This research is supported by a grant from the Ministry of Land, Infrastructure and Transport (Grant number: 13TLRP-C067560-05-000000).

REFERENCES

- [1] T. Seiyama, Editor, *Chemical Sensor Technology*, vol. 1, Kodansha LTD and Elsevier, Tokyo, (1988).
- [2] J.H. Yoon and J.S. Kim, "Study on the MEMS-type gas sensor for detecting a nitrogen oxide gas", *Solid State Ionics*, 192, 668-671, (2011).
- [3] B.J. Kim and J.S. Kim, "Gas sensing characteristics of MEMS gas sensor arrays in binary mixed-gas system", *Mater. Chem. Phys.*, 138, 366-374, (2013).
- [4] S.E. Moon, H.K. Lee, N.J. Choi, J. Lee, C.A. Choi, W.S. Yang, J. Kim, J.J. Jong, and D.J. Yoo, "Low power consumption micro C₂H₅OH gas sensor based on micro-heater and screen printing technique", *Sens. Actuators B*, 187, 598-603, (2013).
- [5] S. Tabata, K. Higaki, H. Ohnishi, T. Suzuki, K. Kunihara, M. Kobayashi, "A micromachined gas sensor based on a catalytic thick film/SnO₂ thin film bilayer and a thin film heater Part 2:

- CO sensing", *Sens. Actuators B*, 109, 190-193, (2005).
- [6] K.C. Kim, S.M. Cho, and H.G. Choi, "Detection of ethanol gas concentration by fuel cell sensors fabricated using a solid polymer electrolyte", *Sens. Actuators B*, 67, 194-198, (2000).
- [7] L. F. Zhu, J.C. She, J.Y. Luo, S.Z. Deng, J.Chen, X.W. Ji, N.S. Xu, "Self-heated hydrogen gas sensors based on Pt-coated $W_{18}O_{49}$ nanowire networks with high sensitivity, good selectivity and low power consumption", *Sens. Actuators B*, 153, 354-360, (2011).
- [8] J. Gao, J.P. Viricelle, C. Pijlat, P. Breuil, P. Vernoux, A. Boreave, and A.G. Fendler, "Improvement of the NO_x selectivity for a planar YSZ sensor", *Sens. Actuators B*, 154, 106-110, (2011).
- [9] J.S. Park, H.C. Cho, and S.H. Yi, "NDIR CO gas sensor with improved temperature compensation", *Procedia Eng.*, 5, 303-306, (2010).
- [10] R. Muda, E. Lewis, S.O'Keeffe, G. Dooly, and J. Clifford, "A compact optical fibre based mid-infrared sensor system for detection of high level carbon dioxide emission in exhaust automotive application", *Procedia Chem.*, 1, 593-596, (2009).
- [11] B. Hök, H. Petterson, A.K. Andersson, S. Hassl, and P. Åkerlund, "Breath analyzer for alcolocks and screening devices", *IEEE Sens.*, 10, 10-15, (2010).
- [12] J.S. Park and S.H. Yi, "Nondispersive infrared rays CH_4 gas sensor using focused infrared beam structures", *Sens. Mater.*, 23, 147-158, (2011).
- [13] S.W. Moon and Y.G. Lim, "NDIR Gas", Korea Patent 101108495000, Jan. 16 (2012).
- [14] H.G.E. Martin, "Gas sensor", U.S. Patent 6,194,735 B1, Feb. 27 (2001).
- [15] H.S. Lim, T.Y. Kim, and J.S. Lee, "Non-dispersive infrared gas analyzer having a lens", Korea Patent 1009596110000, May 17 (2010).